Optik 127 (2016) 3082–3085

Contents lists available at ScienceDirect

Optik

journal homepage: www.elsevier.de/ijleo

A graphene saturable absorber for a Tm:YLF pumped passively Q-switched Ho:LuAG laser

Zheng Cui*, Bao-Quan Yao, Xiao-Ming Duan, Ying-Yi Li, Jin-He Yuan, Tong-Yu Dai

National Key Laboratory of Tunable Laser Technology, Harbin Institute of Technology, Harbin 150001, People's Republic of China

ARTICLE INFO

Article history:
Received 30 June 2015
Accepted 5 December 2015

Keywords:
Ho:LuAG
Graphene
Passively Q-switched laser

PACS:
42.55.Rz, 78.67.Wj, 42.60.Gd

ABSTRACT

A passively Q-switched Ho:LuAG solid-state laser using a graphene saturable absorber pumped by a continuous-wave diode-pumped Tm:YLF laser was first reported in this letter. Single layer graphene grown by chemical vapor deposition and transferred onto a thin quartz plate was fabricated as the SA. For the continuous-wave mode, a maximum output power of 0.87 W at 2100.7 nm was obtained under the output coupler $T = 10\%$, corresponding to the slope efficiency of 30.8% and the optical conversion efficiency of 18.9%. For the passively Q-switched mode, a stable PQS Ho:LuAG laser under the highest incident pump power of 4.3 W was obtained, corresponding to the maximum average output power, the maximum repetition frequency and the minimum pulse width being 0.37 W, 48.8 kHz and 752.2 ns, respectively. Our results illustrate that graphene can be used well as a saturable absorber in a Ho-doped solid-state laser at 2 μm wavelength.

1. Introduction

2 μm Q-switched solid-state lasers operating in the eye-safe wavelength region have various applications, including micro-machining and materials processing [1], environmental gas monitoring [2], optoelectronic countermeasures [3], and coherent Doppler wind lidars [4,5]. In particular, the 2 μm laser plays a pivotal role in achieving the long- wave infrared output as it's efficient pump source of optical parametric oscillators (OPOs) and optical parametric amplifiers (OPAs) [6]. In recent years, the applications of holmium-doped 2 μm lasers in these areas are very significant with the development of 1.9 μm laser pump sources. Due to the low inherent quantum defect between the pump laser and output laser, the resonant pumped holmium- doped laser has many advantages, including a high quantum efficiency and minimal heating, etc. What's more, because of the larger emission cross section and long upper lifetime, holmium-doped solid-state lasers are very suitable for generating nanosecond pulse and high peak power laser output with Q-switching operation. Passively Q- switched (PQS) lasers, which have the advantages of small size of the system, simple design and low cost, are very useful in a lot of areas. However, in the results of the limitation of saturable absorbers (SAs) at 2 μm wavelength, most of recent research has been focused on active Q- switching holmium-doped lasers with acoustic optical (AO) modulators [7].

Graphene is a single layer film of carbon atoms, the carbon atoms are arranged in a hexagonal honeycomb shape on a plane. Due to graphene with very thin thickness, broadband saturable absorption, excellent thermal performance, and low cost, it has significant potential advantages compared to the traditional PQS crystals (Cr:YAG, SESAM, Cr:ZnSe, GaAs, etc.) [8–10]. So far, PQS lasers using graphene as a SA have been widely reported in the wavelength range of 1.123 μm, 1.34 μm, and 1.645 μm [11–13]. By virtue of the ultra-broadband saturable absorption, graphene becomes an excellent SA for 2 μm region. However, most of these studies focused on Thulium-doped lasers [14,15], and holmium-doped lasers have rarely been reported[16].

In this paper, we demonstrated the performances of a continuous-wave (CW) and PQS Ho:LuAG solid-state laser using a graphene as a SA. The graphene grown by a chemical vapor deposition (CVD) process and transferred onto a thin quartz plate was successfully fabricated as the SA. For the CW mode, a maximum output power of 0.87 W at 2100.7 nm with a slope efficiency of 30.8% and the optical conversion efficiency of 18.9% was achieved under the output coupler $T = 10\%$. For the PQS mode, a maximum average output power of 0.37 W with a repetition rare of 48.8 kHz and a pulse width of 752.2 ns under the highest incident pump power of 4.3 W was obtained under the output coupler $T = 10\%$. As far as we know, this is the first time to obtain PQS Ho:LuAG solid-state lasers at 2 μm by using a single layer graphene SA.

* Corresponding author. Tel.: +86 15946094216; fax: +86 0451 86412720.
E-mail address: cuizheng3333@163.com (Z. Cui).

http://dx.doi.org/10.1016/j.ijleo.2015.12.086
0030-4026/

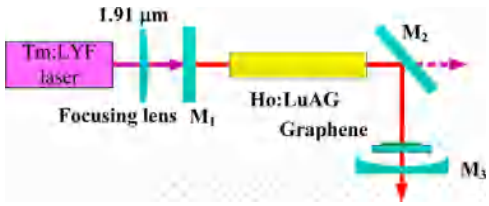

Fig. 1. Experiment setup of the PQS Ho:LuAG laser.

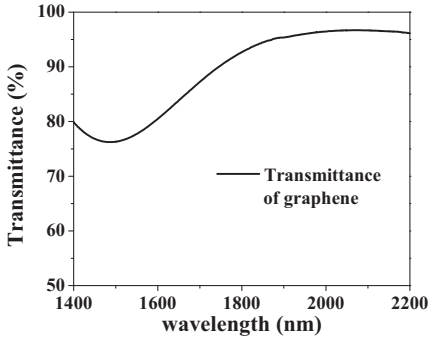

Fig. 2. Typical transmission spectrum of graphene SA.

2. Experiment setup

The geometry of the Ho:LuAG laser resonance pumped by Tm:YLF was shown in Fig. 1. The pump source was a Tm:YLF laser at 1907.6 nm with the maximum output power of 10 W and the M^2 factor of 2.4. The pump beam was focused into the gain medium by a 100 mm focal length lens to a spot radius of 0.16 mm ($1/e^2$ intensity) measured in the air at the position of gain crystal. A Ho:LuAG crystal, with size of Φ5 mm × 30 mm and 0.5 at.% Ho^{3+} concentration, was used as the gain medium. Both ends of the crystal coated at 1.91 μm ($R < 0.5\%$) and 2.1 μm ($R < 0.3\%$) anti-reflection (AR) film. The crystal was wrapped with indium foil and mounted with a water-cooled copper heat sink maintaining at a temperature of 17 °C. The length of the Ho:LuAG laser resonator was 70 mm, using L-shaped configuration. The laser cavity was formed by a flat mirror (M1) and a 45° dichroic mirror (M2) with high transmission ($T > 99.8\%$) at 1.91 μm and high reflectivity ($R > 99.8\%$) at 2.1 μm, and a plane-concave output coupler (M3). M3 was the output coupler, which had a transmission of 2% or 10% at 2.1 μm with a curvature radius of 100 mm. The beam radius of the Ho:LuAG laser inside the resonator was calculated. In the middle of the Ho:LuAG crystal, the radius of the oscillating mode was about 188.5 μm, and the radius of the

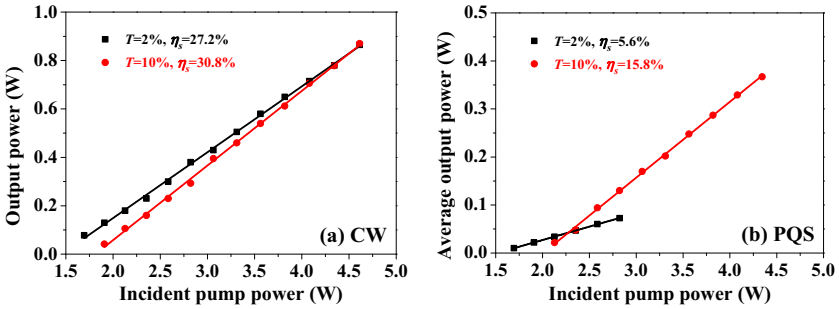

Fig. 3. Output power versus incident pump power: (a) CW (b) PQS operations.

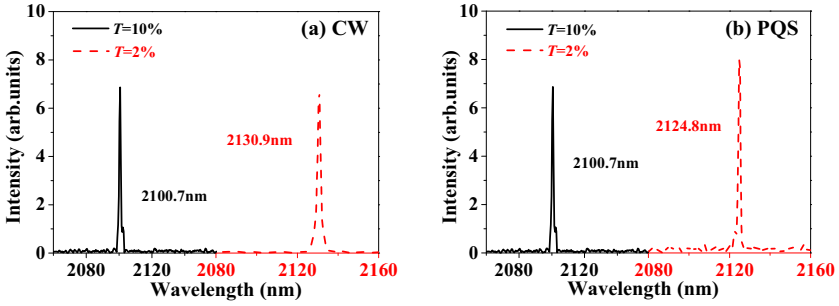

Fig. 4. Laser spectra in (a) CW and (b) PQS operations.

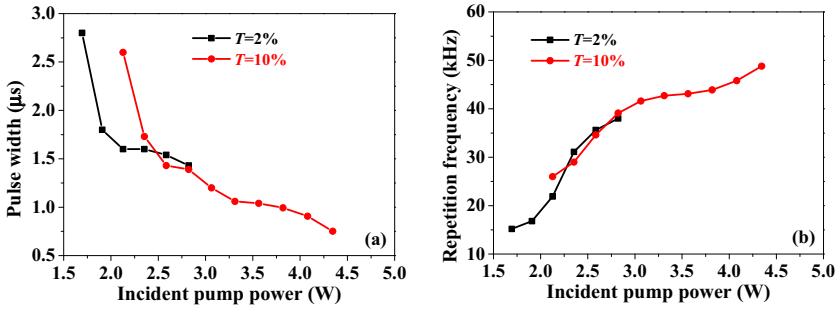

Fig. 5. (a) Pulse width and (b) pulse repetition frequency versus incident pump power.

oscillating mode on the graphene SA was about 250 μm. For PQS operation, we chose the graphene SA produced by CVD for our experiment. End of the graphene SA coated at 2.1 μm ($R < 0.3\%$) AR film. The transmission spectrum of graphene SA was measured with a JASCO V-570 type ultraviolet/visible/near-IR spectrophotometer with a resolution of 0.4 nm. Typical transmission spectra of graphene SA is shown in Fig. 2. As shown in Fig. 1, the graphene SA had high transmission ($T > 96\%$) in the long- wavelength region (1950–2200 nm), so it can be used well as the SA in most 2 μm solid-state lasers with low insert loss. The dimension of the graphene SA was $7 \times 7\ mm^2$ in cross section. The thickness of the graphene was single layer [17–19]. The laser pulse was recorded by a Lecroy digital oscilloscope (Wavesurfer 64 Xs, 2.5 G-samples/s, 600 MHz bandwidth) with an InGaAs detector. The average output power was measured by a power meter (COHERENT PM30 and PM2). The spectra were measured with a Spectrum Analyzer (BRISTOL INSTRUMENTS 721).

3. Experiment results and discussion

Fig. 3(a) shows the change of the output power of CW Ho:LuAG with the incident pump power for different output couplers with the $T = 2\%$ and $T = 10\%$. Straight lines were the results of a linear fit, and the calculated slope efficiencies were given in Fig. 3(a). As shown in Fig. 3(a), the best result was obtained when the output coupler the $T = 10\%$ was used. A highest output power of 0.87 W was obtained at the incident pump power of 4.6 W, corresponding to the slope efficiency of 30.8%. When the output coupler is changed to $T = 2\%$, the maximum output powers of 0.86 W are obtained with the slope efficiency of 27.2%. The output characteristic of the PQS Ho:LuAG was investigated by inserting the graphene SA into the cavity. The average output power as a function of incident pump power with three different output couplers mentioned above was shown in Fig. 3(b). As can be observed from Fig. 3(b), the average output power increased linearly with the incident pump power, and the best result was obtained from the $T = 10\%$. Under the incident pump power of 4.3 W, the highest average output power of 0.37 W with a slope efficiency of 15.8% was obtained. For the output couplers of the $T = 2\%$, the highest average output powers of 0.07 W are obtained with the slope efficiency of 5.6%, corresponding to the incident pump power of 2.8 W. If increase in the incident power pump, we found that bad point on the face of graphene, and unstable pulse train by the oscilloscope observation. The damage threshold of the saturable absorber was approximately $18.7\ W/mm^2$. Moreover, a Glan prism was used to detect output laser polarization state, and then vertically polarized output light was found.

Fig. 4 shows the laser spectra recorded at the incident pump power of 2.6 W. For the CW operation, as can be found from Fig. 4(a), there were two different centric wavelength of 2100.7 nm and 2130.9 nm for two different output couplers mentioned above with the spectral width of 1.1 nm and 1.7 nm. The laser centric wavelength was depended on the transmittance of output coupler, and shortened when increasing the transmittance. For the PQS operation, the output centric wavelength shifted to the shorter wavelength of 2124.8 nm with the spectral width of 1.0 nm when the above output coupler with 2% transmission was used as shown in Fig. 4(b). The output centric wavelength was still 2100.7 nm with the spectral width of 1.3 nm for the output coupler with transmittance of 10%, as same in CW mode. The shift of the central wavelength resulted from the varied resonator loss with the transmission of output coupler and the changing emission cross-section at the different position of emission peak. For the $T = 2\%$ output coupler, the inversion population density was very high when the laser pulse began to build as a result of the intracavity losses increased greatly when inserting the graphene SA into the cavity, which

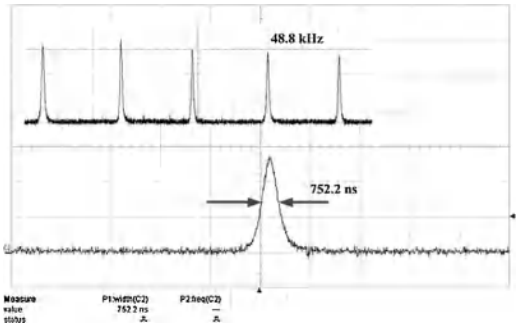

Fig. 6. Output coupler of $T = 10\%$, Pulse profile with duration of 752.2 ns, the inset shows pulse train with a repetition frequency of 48.8 kHz.

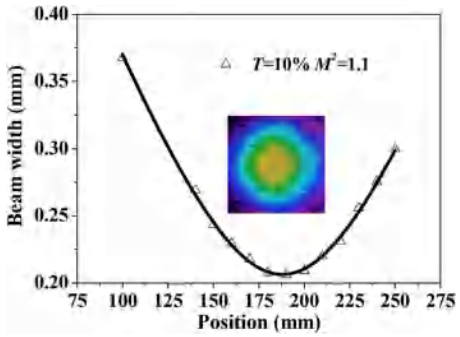

Fig. 7. Output coupler of $T = 10\%$, far field beam profile and the result of M^2 measurement.

resulted in the output central wavelength under the PQS operation blue-shifting relative to the CW operation. When the transmission of the output coupler is equal to 10%, the Ho:LuAG crystal has the strongest emission cross-section at 2097 nm and is larger than the value at 2077 nm and 2025 nm [20]. So, the output wavelength at the PQS operation and CW operation stained same. Addition, the central wavelength is unchanged with the increase of the incident pump power.

Fig. 5(a) showed the pulse width as a function of the incident pump power. From fig. 5(a), the pulse width decreased from 2.8 μs to 1.43 μs, and 2.6 μs to 752.2 ns for different output couplers of the $T = 2\%$ and $T = 10\%$, respectively. It can be seen that the pulse width almost decreased as the incident pump power increased. With the increase of the incident pump power, the inversion population of the gain increased, when the graphene SA is saturable, the photon in the resonator increased sharply to result in the shorter pulse width. Fig. 5(b) shows the pulse repetition frequency versus the incident pump power for different output couplers. For the two output couplers of the $T = 2\%$ and $T = 10\%$, the pulse repetition increased with the incident pump power increasing, which were shifted from 15.2 kHz to 38 kHz, and 26 kHz to 48.8 kHz, respectively. It can be seen that the repetition frequency increased as the incident pump power increased. With the increase of the incident pump power, the inversion population of the gain medium increased to generate larger gain to result in the shorter bleaching time for graphene SA which increased the pulse repletion rate. Through the above analysis, it was found that the pulse width and pulse repetition frequency of the Ho:LuAG laser could be effectively controlled by changing the output coupler and the incident pump power.

The output pulse train and a single pulse of the Ho:LuAG laser for the $T = 10\%$, the maximum incident pump power of 4.3 W were shown in Fig. 6. As can be seen from the Fig. 6, the shortest pulse width and pulse repetition frequency were 752.2 ns and 48.8 kHz. The transverse output beam profile is measured by using 90/10 knife-edge technique. The M^2 factor was calculated to be 1.1. It can

be seen from Fig. 7 that the output beam was close to fundamental transverse electromagnetic mode (TEM_{00}).

4. Conclusion

In this paper, we demonstrated a resonant pumped CW and PQS Ho:LuAG laser. The influence of different output couplers on laser performances was investigated. A maximum CW output power of 0.87 W at 2100.7 nm was achieved when the output coupler was T = 10%, corresponding to a slope efficiency of 30.8% and the optical conversion efficiency of 18.9%. With a graphene SA inserted into the cavity, the central wavelength was 2100.7 nm for the 10% transmission output coupler, as same in CW mode. For the 2% transmission output coupler, the central wavelength shifted from 2130.9 nm to 2124.8 nm. Furthermore, a maximum average output of 0.37 W, and the highest pulse repetition frequency of 48.8 kHz, and a minimum pulse width of 752.2 ns were obtained by used the output coupler of T = 10%.

Acknowledgements

This work was supported by National Natural Science Foundation of China (Nos. 61308009, 61405047), Fundamental Research funds for the Central Universities (Grant Nos. HIT. NSRIF. 2014044, HIT. NSRIF. 2015042), and Science Fund for Outstanding Youths of Heilongjiang Province (JQ201310).

References

[1] M.C. Gower, Industrial applications of laser micromachining, Opt. Express 7 (2) (2000) 56–67.
[2] M.W. Sigrist, Trace gas monitoring by laser photoacoustic spectroscopy and related techniques (plenary), Rev. Sci. Instrum. 74 (1) (2003) 486–490.
[3] G. Renz, W. Bohn, Two-micron thulium-pumped-holmium laser source for DIRCM applications, Proc. SPIE 6552 (2007) 655202.
[4] S.W. Henderson, P.J.M. Suni, S.M. Hannon, J.R. Magee, D.L. Bruns, E.H. Yuen, Coherent laser radar at 2 μm using solid-state lasers, IEEE Trans. Geosci. Remote Sens. 31 (1) (1993) 4–15.
[5] G.J. Koch, B.W. Barnes, M. Petros, J.Y. Beyon, F. Amzajerdian, J. Yu, R.E. Davis, S. Vay, M.J. Kavaya, U.N. Singh, Coherent differential absorption lidar measurements of CO_2, Appl. Opt. 43 (26) (2004) 5092–5099.
[6] A.S. Kurkov, V.A. Kamynin, E.M. Sholokhov, A.V. Marakulin, Mid-IR supercontinuum generation in Ho-doped fiber amplifier, Laser. Phys. Lett. 8 (10) (2011) 754–757.
[7] Y.J. Shen, B.Q. Yao, X.M. Duan, G.L. Zhu, W. Wang, Y.L. Ju, Y.Z. Wang, 103 W in-band dual-end-pumped Ho:YAG laser, Opt. Lett. 37 (17) (2012) 3558–3560.
[8] F. Bonaccorso, Z. Sun, T. Hasan, A.C. Ferrari, Graphene photonics and optoelectronics, Nat. Photonics 4 (2010) 611–622.
[9] M. Liu, X.B. Yin, E.U. Avila, B.S. Geng, A graphene-based broadband optical modulator, Nature 474 (2011) 64–67.
[10] W.D. Tan, C.Y. Su, R.J. Knize, G.Q. Xie, L.J. Li, D.Y. Tang, Mode locking of ceramic Nd:yttrium aluminum garnet with graphene as a saturable absorber, Appl. Phys. Lett. 96 (3) (2010) 031106.
[11] S.J. Men, Z.J. Liu, X.Y. Zhang, Q.P. Wang, H.B. Shen, F. Bai, L. Gao, X.G. Xu, R.S. Wei, X.F. Chen, A graphene passively Q-switched Nd:YAG ceramic laser at 1123 nm, Laser. Phys. Lett. 10 (3) (2013) 035803.
[12] J.L. Xu, X.L. Li, J.L. He, X.P. Hao, Y. Yang, Y.Z. Wu, S.D. Liu, B.T. Zhang, Efficient graphene Q-switching and mode locking of 1.34 μm neodymium lasers, Opt. Lett. 37 (13) (2012) 2652–2654.
[13] Z.X. Zhu, Y. Wang, H. Chen, H.T. Huang, D.Y. Shen, J. Zhang, D.Y. Tang, A graphene-based passively Q-switched polycrystalline Er:YAG ceramic laser operating at 1645 nm, Laser. Phys. Lett. 10 (5) (2013) 055801.
[14] M. Jiang, H.F. Ma, Z.Y. Ren, X.M. Chen, J.Y. Long, M. Qi, D.Y. Shen, Y.S. Wang, J.T. Bai, A graphene Q-switched nanosecond Tm-doped fiber laser at 2 μm, Laser Phys. Lett. 10 (5) (2013) 055103.
[15] Q. Wang, H. Teng, Y. Zou, Z. Zhang, D. Li, R. Wang, C. Gao, J. Lin, L. Guo, Z. Wei, Graphene on SiC as a Q-switcher for a 2 μm laser, Opt. Lett. 37 (3) (2012) 395–397.
[16] C.J. Jin, X.M. Chen, L.F. Li, M. Qi, Y. Bai, Z.Y. Ren, J.T. Bai, A graphene-based passively Q-switched Ho:YAG laser in-band pumped by a diode-pumped Tm:YLF solid-state laser, Laser Phys. 24 (3) (2014) 035801.
[17] R.R. Nair, P. Blake, A.N. Grigorenko, K.S. Novoselov, T.J. Booth, T. Stauber, N.M.R. Peres, A.K. Geim, Fine structure constant defines visual transparency of grapheme, Science 320 (5881) (2008) 1308.
[18] M. Qi, Z.Y. Ren, Y. Jiao, Y.X. Zhou, X.L. Xu, W.L. Li, J.Y. Li, X.L. Zheng, J.T. Bai, Hydrogen kinetics on scalable graphene growth by atmospheric pressure chemical vapor deposition with acetylene, J. Phys. Chem. C 117 (27) (2013) 14348–14353.
[19] A.C. Ferrari, J.C. Meyer, V. Scardaci, C. Casiraghi, M. Lazzeri, F. Mauri, S. Piscanec, D. Jiang, K.S. Novoselov, S. Roth, A.K. Geim, The Raman fingerprint of graphene, Phys. Rev. Lett. 97 (2006) 187401.
[20] B.Q. Yao, X.M. Duan, L. Ke, Y.L. Ju, Y.Z. Wang, G.J. Zhao, Q-switched operation of an in-band-pumped Ho:LuAG laser with kilohertz pulse repetition frequency, Appl. Phys. B 98 (2–3) (2010) 311–315.